MATCH
Communications in Mathematical and in Computer Chemistry

MATCH Commun. Math. Comput. Chem. **95** (2026) 441–456
ISSN: 0340–6253
doi: 10.46793/match.95-2.11925

The Sweep Method as One of the Methods for Solving the Charge Transport Problem in an Alkaline Electrolyte

Violetta Chebakova[a,b,*], **Lenar Kashapov**[a,b], **Nail Kashapov**[b,c], **Maksim Dmitriev**[a]

[a] *Kazan (Volga Region) Federal University, Kremlevskaya ul. 18, Kazan, Country, Kazan*

[b] *Tatarstan Academy of Sciences, Institute of Applied Research of Tatarstan Academy of Sciences, Bauman str, 20, Kazan, 420111, Russia*

[c] *Institute of Mechanics and Engineering, FRC Kazan Scientific Center, Russian Academy of Sciences, Kazan, Russia*

vchebakova@mail.ru, kashlenar@mail.ru, kashnail@gmail.com, dmitmax2002@yandex.ru

(Received May 19, 2025)

Abstract

Metallic zinc-based alloys are being extensively investigated for potential use in medicine for the fabrication of implants via additive manufacturing technologies. A mathematical model for zinc electro-extraction from a 20% sodium hydroxide solution is proposed. The initial–boundary–value problems for charged-particle transport that describe the electrolysis processes possess several features that complicate their numerical solution. Was developed and proposed a modification of the streamline-sweep method, suitable for the charged-particle transport problem in an electrolyte when a convective term and variable coefficients are present. This method

*Corresponding author.

computes the charged-particle flux at the same time as the primary solution. This approach avoids the large errors that occur when flux is obtained by numerically differentiating the solution. The algorithm was verified by comparison with experimental data and with the results of solving a one-dimensional kinetic problem at the electrode. The one-dimensional model treats both diffusive and drift fluxes more accurately than the kinetic model. As a result, the initial-stage discrepancy between experimental data and computed results was cut by 50 %.

1 Introduction

Zinc-based metallic alloys are extensively studied for potential. The feasibility of using zinc and its alloys for implant manufacturing has been investigated in studies [3, 18]. Traditional manufacturing processes for producing customized implants, such as porous scaffolds for tissue engineering, face significant limitations. Study [11] describes the laser powder bed fusion (L-PBF) technique as a reliable method for fabricating metallic implants from zinc-based alloys. This additive manufacturing approach enables the production of implants with a personalized structure tailored to meet the specific needs of the patient. Additionally, the influence of alloy composition on corrosion, which increases Zn^{2+} concentration in bone tissue and may potentially inhibit bone regeneration, has been investigated. Study [13] provides a review of 3D printing methods for manufacturing patient-specific orthopedic implants from biomaterials and metals. Zinc-based alloys are recommended for the production of bone screws and load-bearing components of bone plates due to zinc's cytotoxicity, absence of gas formation, and high biocompatibility. However, pure zinc is rarely used due to its low mechanical strength, and zinc-based alloys with additional metallic elements (e.g., Mg, Ca, and Sr) are more commonly employed. Study [15] presents research on the physicochemical and biological effects of zinc doping in wollastonite bioceramics used for ocular prostheses. Experimental results demonstrated that substituting part of the calcium content with zinc (up to 9%) significantly improves sinterability and mechanical properties. Study [14] highlights the application of zinc-based alloys in the selective laser melting (SLM) fabrication of cardiovascular

stents and dental implants. One of the methods for obtaining pure zinc from low-grade and polymetallic ores or metallurgical waste is electroextraction. Electroextraction also recovers cadmium, indium, gallium, and other metals from polymetallic ores. The electrochemical system of the electroextraction process consists of a cathode, an electrolyte, and an insoluble anode. The solutions used are typically obtained through selective dissolution (leaching) of metal-containing ores, ore concentrates, or intermediate metallurgical products. In this study, a mathematical model of zinc electroextraction from a 20% sodium hydroxide solution is proposed. The mathematical model is developed for the deposition of a porous zinc layer. In this case, the zinc evolution process is governed by diffusion toward the electrode. The process rate can be considered proportional to the diffusion flux and inversely proportional to the thickness of the deposited zinc layer. The peculiarities of the electrolysis process, which complicate the numerical solution of this model, are described. Additionally, a modified sweep method for solving the model is proposed and substantiated.

2 Mathematical description of the zinc electroextraction process from low-grade ore

2.1 Equations in the electrolyte volume

The explanation of the mathematical model for the zinc electroextraction process from an alkaline electrolyte is provided in study [7]. The mathematical model is constructed for ore leaching with a solution containing 20% sodium hydroxide. According to [19], a sodium hydroxide concentration of 20% is sufficient for the overall dissolution reaction $2NaOH + Zn + 2H_2O \rightarrow Na_2[Zn(OH)_4] + H_2$ whereas at lower $NaOH$ concentrations the reaction proceeds with formation of zinc oxide (ZnO). For the experiment, as in study [7], the preparation of the electrolyte is carried out by leaching zinc from the ore using a sodium hydroxide solution (20%) with the overall reaction $2NaOH + Zn + 2H_2O \rightarrow Na_2[Zn(OH)_4] + H_2$ sodium tetrahydroxo zincate completely dissociates into ions in the solution [19, 20]

$$Na_2[Zn(OH)_4] \rightarrow 2Na^+ + [Zn(OH)_4]^{2-}.$$

The mathematical model is posed between flat parallel inert electrodes with an inter-electrode distance greater than the geometric dimensions of the electrode. The mathematical model contains the following second-order differential equations:

1. The diffusion-convection equation for hydrogen ions is as follows

$$\frac{\partial C_{H^+}}{\partial t} + \frac{\partial}{\partial x}\left(-D_{H^+}\frac{\partial C_{H^+}}{\partial x} + U_{H^+}C_{H^+}\frac{\partial \varphi}{\partial x}\right) = \\ = R_1 C_{H_2O} - R_2 C_{OH^-} C_{H^+} \quad (1)$$

Here, C_{H^+} is the concentration of hydrogen ions, D_{H^+} is the diffusion coefficient of hydrogen ions, U_{H^+} is the mobility coefficient of hydrogen ions,φ is the electric field potential,R_1 is the water dissociation constant, and R_2 is the association constant of hydroxide ions and hydrogen ions into a water molecule.

2. The diffusion-convection equation for the hydroxide group

$$\frac{\partial C_{OH^-}}{\partial t} + \frac{\partial}{\partial x}\left(-D_{OH^-}\frac{\partial C_{OH^-}}{\partial x} - U_{OH^-}C_{OH^-}\frac{\partial \varphi}{\partial x}\right) = \\ = R_1 C_{H_2O} - R_2 C_{OH^-} C_{H^+} \quad (2)$$

Here, C_{OH^-} is the concentration of hydroxide ions, D_{OH^-} is the diffusion coefficient of hydroxide ions, and U_{OH^-} is the mobility coefficient of hydroxide ions.

3.The diffusion-convection equation for sodium ions

$$\frac{\partial C_{Na^+}}{\partial t} + \frac{\partial}{\partial x}\left(-D_{Na^+}\frac{\partial C_{Na^+}}{\partial x} + U_{Na^+}C_{Na^+}\frac{\partial \varphi}{\partial x}\right) = 0 \quad (3)$$

Here, C_{Na^+}, D_{Na^+}, U_{Na^+} represent the concentration, diffusion coefficient, and mobility coefficient of sodium ions, respectively.

4. The diffusion-convection equation for tetrahydroxozincate anions

$$\frac{\partial C_{[Zn(OH)_4]^{2-}}}{\partial t} + \frac{\partial}{\partial x}\left(-D_{[Zn(OH)_4]^{2-}}\frac{\partial C_{[Zn(OH)_4]^{2-}}}{\partial x}\right) \\ -\frac{\partial}{\partial x}\left(U_{[Zn(OH)_4]^{2-}}C_{[Zn(OH)_4]^{2-}}\frac{\partial \varphi}{\partial x}\right) = 0 \quad (4)$$

Here, $C_{[Zn(OH)_4]^{2-}}$,$D_{[Zn(OH)_4]^{2-}}$, $U_{[Zn(OH)_4]^{2-}}$ represent the concentration, diffusion coefficient, and mobility coefficient of tetrahydroxozincate anions, respectively.

5. The Poisson equation, in the approximation of its potentiality and homogeneity along the electrodes

$$\frac{1}{F}\frac{\partial((1+\chi)\varepsilon_0 E)}{\partial x} = (C_{Na^+} + C_{H^+} - C_{[Zn(OH)_4]^{2-}} - C_{OH^-}) \qquad (5)$$

Here, χ is the electric susceptibility of the medium,ε_0 is the dielectric constant, F is Faraday's constant, and $E = -\frac{\partial\varphi}{\partial x}$ is the electric field intensity.

6. The boundary conditions The equation for water molecules in general form is written as:

$$\frac{\partial C_{H_2O}}{\partial t} + \frac{\partial}{\partial x}\left(-D_{H_2O}\frac{\partial C_{H_2O}}{\partial x}\right) = R_1 C_{H_2O} - R_2 C_{OH^-} C_{H^+} \qquad (6)$$

However, since the dissociation and association constants of water are very small, and the transport of water does not affect charge transport, we will consider the water concentration as constant when solving the model problem The ion product of water $K_W = C_{H^+}C_{OH^-}$ remains constant under unchanged conditions. The mobility of ions U can be expressed through the equivalent conductivity Λ as:$\Lambda = UF$

2.2 The boundary conditions at the cathode and anode

Electrolysis is a heterogeneous process, and the main reactions occur at the phase boundary, specifically between the surface of the liquid electrolyte and the metal electrode. These reactions depend on the pH of the medium. In an alkaline environment oxygen evolves at the anode. In alkaline media hydrogen adsorption at the cathode proceeds via $H_2O + 2e \rightarrow O + 2H^+$, and oxygen evolution at the anode via $2OH^- \rightarrow O + H_2O$. At the cathode, the hydrogen-evolution reaction runs in parallel with zinc deposition. There is, however, debate about the precise interfacial mechanism of zinc deposition. It has been suggested that during electrodeposition the $[Zn(OH)_4]^{2-}$ complex is converted into hydrated $Zn(OH)_2$. Since zinc hydroxide is an insoluble base, one would expect to de-

tect it in the cathodic deposit; yet most studies do not observe it [12] . Thus, at the cathode the following stepwise reactions take place: $[Zn(OH)_4]^{2-} \xrightarrow{k_1} Zn^{2+} + 4OH^-$, $Zn^{2+} + 2e \xrightarrow{k_2} Zn$, $H_2O \xrightarrow{k_3} H^+ + OH^-$, $H^+ + OH^- \xrightarrow{k_4} H_2O$, $H^+ + e \xrightarrow{k_5} H$, $H + H \xrightarrow{k_6} H_2$. At the anode, water decomposition proceeds via the sequence [9]:$H_2O \xrightarrow{l_1} H^+ + OH^-$, $H^+ + OH^- \xrightarrow{l_2} H_2O$, $2OH^- + 2e \xrightarrow{l_3} O + H_2O$, $O + O \xrightarrow{l_4} O_2$. Here, k_1, k_2, k_3, k_4, k_5, k_6 are the rate constants for the various stages of the electrochemical reactions, l_1, l_2, l_3, l_4 are the rate constants for the anodic pre-electrode electrochemical reactions. The mathematical description of the cathodic processes is expressed by the system of kinetic equations:

$$\begin{cases} \partial C_{H_2O}/\partial t = -k_3 C_{H_2O}, \\ \partial C_{H^+}/\partial t = k_3 C_{H_2O} - k_5 C_{H^+}, \\ \partial C_H/\partial t = k_5 C_{H^+} - k_6 C_H C_H, \\ \partial C_{H_2}/\partial t = k_6 C_H C_H, \\ \frac{\partial C_{[Zn(OH)_4]^{2-}}}{\partial t} = -D_{[Zn(OH)_4]^{2-}} \frac{\partial C_{[Zn(OH)_4]^{2-}}}{\partial x} k_7 - k_1 C_{[Zn(OH)_4]^{2-}}, \\ \partial C_{Zn^{2+}}/\partial t = k_1 C_{[Zn(OH)_4]^{2-}} - k_2 C_{Zn^{2+}}, \\ \partial C_{Zn}/\partial t = k_2 C_{Zn^{2+}}, \end{cases} \tag{7}$$

The rate constants for the stage processes at the electrode are calculated based on the works [1, 2, 8].The method for calculating the interfacial-process rate constants from [9] allows the electrochemical reactions at each electrode to be treated separately. Additionally, taking into account the results of work [9], where k_4 was practically zero, this stage process is not considered in the present system. Sodium ions do not undergo deposition at the cathode; rather, their redistribution occurs in the interelectrode space, with an increase in concentration near the cathode and a decrease near the anode. For sodium ions, we impose a continuity condition on the

flux, considering that convection outweighs diffusion.

$$C_{Na^+}|_{cathode} = U_{Na^+} C_{Na^+} \frac{\partial \varphi}{\partial x}, \tag{8}$$

For the Poisson equation, the boundary condition at the cathode is set based on the Nernst equation:

$$\varphi|_{cathode} = E_{0,cathode} + \frac{RT}{F} \ln \left(\frac{C_{H^+} C_{Zn^+}}{C_H} \right) \tag{9}$$

The mathematical description of the anodic processes is expressed by the system of kinetic equations:

$$\begin{cases} \frac{\partial C_{H_2O}}{\partial t} = & -l_1 C_{H_2O} + l_2 C_{H^+} C_{OH^-} + l_3 C_{OH^-}^2 \\ \frac{\partial C_{OH^-}}{\partial t} = & l_1 C_{H_2O} - l_2 C_{H^+} C_{OH^-} - l_3 C_{OH^-}^2 \\ \frac{\partial C_O}{\partial t} = & l_3 C_{OH^-}^2 - l_4 C_O^2 \\ \frac{\partial C_{O_2}}{\partial t} = & l_4 C_O^2 \\ \frac{\partial C_{H^+}}{\partial t} = & -l_1 C_{H_2O} + l_2 C_{H^+} C_{OH^-} \end{cases} . \tag{10}$$

The concentration of sodium ions in the anodic space is assumed to be zero:

$$C_{Na^+}|_{anode} = 0. \tag{11}$$

For the Poisson equation, the boundary condition at the anode is also set based on the Nernst equation:

$$\varphi|_{anode} = E_{0,anode} + \frac{RT}{F} \ln \left(\frac{1}{C_{OH^(-)}} \right) \tag{12}$$

For tetrahydroxozincate anions, the Nernst boundary condition can be written as:

$$C_{[Zn(OH)_4]^{2-}}|_{anode} = (U_{[Zn(OH)_4]^{2-}})(C_{[Zn(OH)_4]^{2-}}) \frac{\partial \varphi}{\partial x}. \tag{13}$$

When an electric current passes through a heterogeneous system consisting of metal electrodes and a liquid electrolyte, the primary processes occur at the phase boundary, where there is a strong concentration imbalance. As we move away from the electrode regions, due to the polarization of the medium, ions become more bound. Due to the smallness of the dissociation and association constants, in this region, the ion concentration is determined solely by diffusion-migration transfer. In the electrode regions, drift processes dominate over diffusion processes, leading to significant changes in characteristics such as concentration and voltage values [6, 17]. Thus, the constructed mathematical model has strong gradients in the solutions of these initial-boundary problems and boundary value problems, which significantly complicates their solution. Also, one of the characteristics for comparing experimental and calculated values is the volt-ampere characteristic (VAC), which is the relationship between the total current through the gas discharge gap and the voltage across it. The total current, which is the sum of the fluxes of all charged particles, must be the same at every point in space within this heterogeneous system.

3 The numerical method for solving

The algorithm sequentially solves charged-particle transport and potential problems. It also solves the boundary Cauchy problem using a fourth-order Runge-Kutta method. The solution algorithm involves the sequential numerical solution of initial-boundary value problems for the transport of charged particles and boundary value problems for determining the potential. In this process, the Cauchy problem is additionally solved at the boundary using the Runge-Kutta method of the fourth order. The construction of a difference scheme for differential equations and the solution of the resulting system of algebraic equations will be considered using the example of the initial-boundary value problem of diffusion-migration of hydrogen ions. This problem, as noted above, has several features that complicate its solution:

1) The large concentration gradients in the near-electrode regions lead to computational errors when numerically calculating the particle flux in

these near-electrode regions.

2) The shift from diffusion-dominated regions in the gap center to convection-dominated near-electrode regions changes the equation type and limits solution methods.

3) The presence of a strong gradient of the electric field in the near-electrode regions leads to the dominance of the convection process. Thus, a problem arises in approximating the first-order derivative when using implicit schemes. The approximation of the central difference derivative may result in a violation of diagonal dominance and, consequently, cause instability in the computations when solving the system of algebraic equations. However, when using upwind differences for the approximation, the order of accuracy of the computations decreases.

Using the standard sweep formula requires numerical differentiation to get the flux, leading to accuracy loss. Therefore, we use a streamline-sweep method adapted for diffusion terms. The classical method (Samarsky [16, 21]) applies only to pure convection equations. For instance, in [4], a variant of the streamline sweep method is proposed for modeling semiconductor devices to solve the electron transport problem. Let's consider the possibility of applying the streamline sweep method to the problem of transporting hydrogen anions during electrolysis, taking into account the convective term and time-varying coefficients in the inter-electrode space. For simplicity, let C represent the concentration of hydrogen ions C_{H^+}, D represent the diffusion coefficient D_{H^+}, u represent the mobility coefficient U_{H^+}, ψ denote the source of hydrogen ions $R_1 C_{H_2O}$, and a represent the product of $R_2 C_{HO^-}$. The initial-boundary value problem for the diffusion-migration of hydrogen ions in general form, including the flux term, can be written as:

$$\frac{\partial C}{\partial t} + \frac{\partial G}{\partial x} = \psi - aC \tag{14}$$

$$G = -D\frac{\partial C}{\partial x} + uEC \tag{15}$$

Here, G is the hydrogen ion flux. The concentration of hydrogen at the cathode ψ_1 and at the anode ψ_2 is found by solving the Cauchy problem

systems (7), (10) using the explicit fourth-order Runge-Kutta method. In the problem we are considering, the boundary conditions will be interpreted as Dirichlet conditions (first-kind conditions).

$$C_{H^+}|_{cathode} = \psi_1. \tag{16}$$

$$C_{H^+}|_{anode} = \psi_2. \tag{17}$$

The formulation of the charged particle balance problem with separate highlighting of the flux is widely used both in gas discharges and in solid conductors [5, 10]. The discretization of equation (14) and the construction of the difference scheme will be carried out using the integral-interpolation method, which is commonly used for constructing conservative difference schemes. For this, we introduce a coordinate system, directing the Ox axis perpendicular to the surface of the electrode, placing the cathode at $x = 0$. The anode will then be located at $x = b$, where b is the diste betweeancn the cathode and the anode. Next, we introduce a spatiotemporal grid $\omega_h \times \omega_t$ on the segment $[0, b]$, where: $\omega_t = \{t_0 = 0, t_j = t_{j-1} + \tau, j = 1, 2, \ldots\}$ Here, h is the spatial step, and τ is the time step. The integral-interpolation method consists of integrating the differential equation over non-intersecting regions surrounding each grid node, and subsequently approximating the integrals. To solve the problem, we define $\omega_{h+1/2} = \{x_{1/2}, \ldots, x_{i-1/2}, \ldots, x_{N-1/2},\}$, where $x_{i-1/2}$ is the midpoint of the interval $[x_i, x_{i-1}]$. When constructing an implicit difference scheme, the values of the differential equation coefficients are taken from the lower time layer t_{s-1} . The equation (14) is integrated over the segment $[x_{i+h/2} - x_{i-h/2}]$, and $t = t_s$ is assumed.

$$\int_{x_{i-1/2}}^{x_{i+1/2}} \frac{\partial C}{\partial t} \partial x + \int_{x_{i-1/2}}^{x_{i+1/2}} \frac{\partial G}{\partial x} \partial x = \int_{x_{i-1/2}}^{x_{i+1/2}} (\psi - aC)\, \partial x \tag{18}$$

The $\int_{x_{i-1/2}}^{x_{i+1/2}} \frac{\partial G}{\partial x} \partial x$ will be expanded using the Newton-Leibniz formula. The integrals $\int_{x_{i-1/2}}^{x_{i+1/2}} \frac{\partial C}{\partial t} \partial x$ and $\int_{x_{i-1/2}}^{x_{i+1/2}} (\psi - aC)\, \partial x$ will be expanded using the quadrature formula of central rectangles.

$$\left.\frac{\partial C}{\partial t}\right|_{x_i} h + G|_{x_{i+1/2}} - G|_{x_{i-1/2}} = (\psi - aC)|_{x_i} h \tag{19}$$

Next, we will use the formulas for numerical differentiation and obtain:

$$\frac{u_i - u_i^0}{\tau} + C_i u_i = \frac{\omega_{i-1/2} - \omega_{i+1/2}}{h} + f_i \tag{20}$$

where u_i, ω_i,C_i,f_i Grid functions, which approximate the values of the solution, flux, source term, and resulting coefficients at the i-th point. The flux (15) will be considered at the grid points $\omega_{h+1/2}$, and the migration term will be approximated using the grid points ω_h:

$$G|_{x_{i-1/2}} = \left(-D\frac{\partial C}{\partial x}\right)\Bigg|_{x_{i-1/2}} + \frac{\omega_{i-1/2} - \omega_{i+1/2}}{h} + f_i \tag{21}$$

Thus, the system of equations (14)-(15) at the grid nodes can be rewritten as follows

$$\frac{u_i - u_i^0}{\tau} + c_i u_i = \frac{\omega_{i-1/2} - \omega_{i+1/2}}{h} + f_i \tag{22}$$

$$\omega_{i-1/2} + d_{i-1/2} u_i = k_{i-1/2} u_{i-1} \tag{23}$$

Where u_i, ω_i, c_i, f_i , $d_{i-1/2}$, $k_{i-1/2}$ are the grid analogs that approximate the values of the solution, flux, source term of the equation, and the resulting coefficients at the i – th point. We assume the existence of a relationship between the unknown function u_{i-1} and the flux $\omega_{i-1/2}$ of the form:

$$\alpha_i u_{i-1} + \beta_i \omega_{i-1/2} = \gamma_i \tag{24}$$

and we find a recurrence relation to compute the sweep coefficients α_i,β_i,γ_i, and the unknown functions u_{i-1},$\omega_{i-1/2}$. To do this, from equation (24), we solve for u_{i-1} and substitute it into equation (23). This gives:

$$\omega_{i-1/2}\left(\alpha_i + k_{i-1/2}\beta_i\right) = k_{i-1/2}\gamma_i - d_{i-1/2}\alpha_i \tag{25}$$

Since the coefficients α_i, β_i, γ_i in equation (24) are determined up to a multiplier, we introduce an additional condition:$\alpha_i + k_(i-1/2)\beta_i = 1$ and

we obtain the final system

$$\omega_{i-1/2} = k_{i-1/2}\gamma_i - d_{i-1/2}\alpha_i u_i \tag{26}$$

Substituting (26) into (22), we get:

$$(c_i + 1/t)\, u_i + \frac{\omega_{i+1/2}}{h} - \frac{k_{i-1/2}\gamma_i - d_{i-1/2}\alpha_i u_i}{h} = f_i + \frac{u_i^0}{t} \tag{27}$$

Now, we group the coefficients of u_{i-1} and obtain:

$$\left(c_i + \frac{1}{t} + \frac{d_{i-1/2}\alpha_i}{h}\right) u_i + \frac{\omega_{i+1/2}}{h} = f_i + \frac{u_i^0}{t} + \frac{k_{i-1/2}\gamma_i}{h} \tag{28}$$

Comparing the resulting equation with equation (24) and considering that, according to [4] , the sufficient stability conditions for the computational process are:

$$\left|\frac{d\alpha_{i+1}}{d\alpha_i}\right| < 1,\ \left|\frac{d\beta_{i+1}}{d\beta_i}\right| < 1,\ \left|\frac{d\gamma_{i+1}}{d\gamma_i}\right| < 1$$

obtain the following recurrence relations: if $\left|d_{i-1/2}\right| \le 1$ and $\left|k_{i-1/2}\right| \le 1$ then $\alpha_{i+1} = c_i + \frac{1}{t} + \frac{d_{i-1/2}\alpha_i}{h}$, $\beta_{i+1} = \frac{1}{h}$, $\gamma_{i+1} = f_i + \frac{u_i^0}{t} - \frac{\gamma_i k_{i-1/2}}{h}$

if $\left|d_{i-1/2}\right| \le 1$ and $\left|k_{i-1/2}\right| > 1$ then $\alpha_{i+1} = \frac{c_i}{k_{i-1/2}} + \frac{1}{tk_{i-1/2}} + \frac{d_{i-1/2}\alpha_i}{hk_{i-1/2}}$, $\beta_{i+1} = \frac{1}{hk_{i-1/2}}$,$\gamma_{i+1} = \frac{f_i}{k_{i-1/2}} + \frac{u_i^0}{tk_{i-1/2}} - \frac{\gamma_i}{h}$

if $\left|d_{i-1/2}\right| > 1$ and $\left|k_{i-1/2}\right| \le 1$ then $\alpha_{i+1} = \frac{c_i}{d_{i-1/2}} + \frac{1}{td_{i-1/2}} + \frac{\alpha_i}{h}$, $\beta_{i+1} = \frac{1}{hd_{i-1/2}}$, $\gamma_{i+1} = \frac{f_i}{d_{i-1/2}} + \frac{u_i^0}{td_{i-1/2}} - \frac{\gamma_i k_{i-1/2}}{hd_{i-1/2}}$ if $\left|d_{i-1/2}\right| > 1$ and $\left|k_{i-1/2}\right| > 1$ then $\alpha_{i+1} = \frac{c_i}{d_{i-1/2}k_{i-1/2}} + \frac{1}{td_{i-1/2}k_{i-1/2}} + \frac{\alpha_i}{hk_{i-1/2}}$, $\beta_{i+1} = \frac{1}{hd_{i-1/2}k_{i-1/2}}$, $\gamma_{i+1} = \frac{f_i}{d_{i-1/2}k_{i-1/2}} + \frac{u_i^0}{td_{i-1/2}k_{i-1/2}} - \frac{\gamma_i}{hd_{i-1/2}}$

To find the recurrence relation for the fluxes, we express u_i from equation (26) and substitute it into equation (22):

if $\left|d_{i-1/2}\right| \le 1$, then

$\omega_{i-1/2} = \left(-\frac{\gamma_i k_{i-1/2}(1+c_i)}{\alpha_i d_{i-1/2} t} + f_i + \frac{u_i^0}{t} + \frac{\omega_{i+1/2}}{h}\right)\left(\frac{h\alpha_i d_{i-1/2}}{1+\alpha_i d_{i-1/2}+c_i}\right)$

if $\left|d_{i-1/2}\right| > 1$, then

$\omega_{i-1/2} = \left(-\frac{\gamma_i k_{i-1/2}(1+c_i)}{\alpha_i d_{i-1/2} t} + f_i + \frac{u_i^0}{t} + \frac{\omega_{i+1/2}}{h}\right)\left(\frac{h\alpha_i}{\frac{1}{d_{i-1/2}}+\alpha_i+\frac{c_i}{d_{i-1/2}}}\right)$

These recurrence formulas are stable with respect to random errors. To compute the sweep coefficients α_1, β_1, γ_1, we will use the boundary con-

ditions at $x = 0$ in the grid analogy. This will give $u_1 = \psi_1$. Comparing with equation (24), we get $\alpha_1 = 1$, $\beta_1 = 0$, $\gamma_1 = \psi_1$. To compute the flux $\omega_{N-1/2}$, we substitute the boundary condition $u_N = f_N$ into equation (24) and solve for $\omega_{N-1/2}$: $\omega_{N-1/2} = \frac{\gamma_n - f_N \alpha_N}{\beta_N}$ The accuracy of the method is determined by the precision of the finite-difference scheme and the determination of the interfacial process constants. An upwind differencing scheme was used to approximate the first derivative, yielding an accuracy of order O(h), where h is the spatial grid step. The procedure for finding these constants is described in [9]. This method was implemented in the MATLAB development environment using custom code written by the authors. During testing of the algorithm, grid convergence was observed when it was evaluated at specific time points. Before applying the electric current, we assume the interelectrode gap is at its initial state [7]. In this state, the Zn^{2+} concentration in the solution is 10 g/L. The working electrode is stainless steel with an area of 1 cm^2 and is assumed inert. The electrolyte is a 20% NaOH solution. We calculated the stage-wise reaction constants using the method from [7] under identical assumptions. Figure 1 compares experimental mass-yield data from [20] with our model's predictions. Both sets of results use the streamwise-sweep method at 125 A. The solution to the model problem based on the data from work [7] showed a quantitative match in the output of zinc. Because the model is formulated in the porous-film approximation, the zero-dimensional kinetic model accounts for the diffusion flux in an approximate form based on the assumption that the process rate is proportional to diffusion and inversely proportional to the thickness of the deposited zinc layer. Its calculations exhibit a large discrepancy during the initial nucleation phase of zinc formation, with convergence of results at later stages. In the one-dimensional model, thanks to a more accurate treatment of both diffusive and drift fluxes, the initial-stage discrepancy was reduced by half: it reached a maximum of 13% at the start and no more than 5% thereafter. Additionally, the qualitative description of the distribution of characteristics in the inter-electrode space was consistent with the physical and electrochemical description.

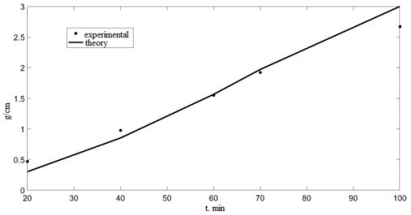

Figure 1. Comparison of zinc yield at a current of 125 A.

4 Conclusion

In this work, a modification of the streamline sweep method is proposed, suitable for the problem of charged particle transport in an electrolyte with the presence of a convective term and varying coefficients. This method allows, along with the solution, to find the value of the flux of charged particles, which helps avoid significant computational errors when calculating the flux using numerical differentiation of the solution. The recurrence formulas for computing the sweep coefficients, the solution, and the flux are stable with respect to random errors. The solution to the model problem showed consistent qualitative results from an electrochemical point of view, including the presence of solution gradients in the near-electrode regions, as well as ion binding in the center of the inter-electrode gap.

***Acknowledgment*:** The work was carried out at the expense of a grant from the Academy of Sciences of the Republic of Tatarstan, provided to young candidates of science (postdoctoral students) for the purpose of defending a doctoral dissertation, carrying out research work, and also performing work functions in scientific and educational organizations of the Republic of Tatarstan within the framework of the State Program of the Republic of Tatarstan "Scientific and Technological Development of the Republic of Tatarstan".

References

[1] V. Chebakova, Modeling of hydrogen release during electrolysis of alkaline solution, *E3S Web Confs.* **592** (2024) #01010.

[2] V.Y. Chebakova, L.N. Kashapov, N.F. Kashapov, Modeling of hydrogen release during electrolysis of alkaline solution, *E3S Web Confs.* **44** (2023) 2607–2612.

[3] K. Chen, X. Gu, Y. Zheng, Feasibility, challenges and future prospects of biodegradable zinc alloys as orthopedic internal fixation implants, *Smart Mater. Manufac.* **2** (2024) #100042.

[4] G. Garber, The use of flux-sweep method for the quasihydrodynamic modeling of semiconductor devices, *Mat. Model.* **1** (1989) 1–7. `https://www.mathnet.ru/rus/mm2632`

[5] G. Z. Garber, A method for calculating the parameters of a small-signal equivalent circuit of microwave heterostructure bipolar transistors with a varizone emitter, based on a quasi-hydrodynamic model of electron transport, *Radio Engin. Elec.* **46** (1997) 1392–1396.

[6] B. S. Haran, B. N. Popov, G. Zheng, R. E. White, Mathematical modeling of hexavalent chromium decontamination from low surface charged soils, *J. Hazard. Mater.* **55** (2001) 93–107.

[7] L. N. Kashapov, N. F. Kashapov, V. Y. Chebakova, E. V. Chebakova, Mathematical modeling of cathodic zinc electroextraction processess, *J. Siberian Federal Univ. Math. Phys.* **16** (2023) 572–582.

[8] L. N. Kashapov, N. F. Kashapov, V. Y. Chebakova, Mathematical simulation of cathode processes during hydrogen production, *Theor. Found. Chem. Engin.* **58** (2024) 595–600.

[9] R. N. Kashapov, L. N. Kashapov, N. F. Kashapov, V. Y. Chebakova, Kinetics of two-phase gas-liquid mediums in electrolysis processes, *High Temp.* **60** (2022) S356–S362.

[10] A. A. Kulikovsky, A more accurate Scharfetter-Gummel algorithm of electron transport for semiconductor and gas discharge simulation, *J. Comput. Phys.* **119** (1995) 149–155. *https* : *//www.sciencedirect.com/science/article/abs/pii/S*00219991 367 − 394367 − 39485711230.

[11] A. Liu, Y. Qin, J. Dai, F. Song, Y. Tian, Y. Zheng, P. Wen, Fabrication and performance of Zinc-based biodegradable metals: From conventional processes to laser powder bed fusion, *Bioactive Mater.* **41** (2024) 312–335.

[12] S. V. Mamyachenkov, S. A. Yakornov, O. S. Anisimova, D. I. Bludova, Review of research results of zinc powder electrolytic production from alkaline solutions, *Ipolytech J.* **23** (2019) 367–394.

[13] M. Meng, J. Wang, H. Huang, X. Liu, J. Zhang, Z. Li, 3D printing metal implants in orthopedic surgery: Methods, applications and future prospects, *J. Orthopedic Trans.* **42** (2023) 94–112.

[14] H. Mobarak, A. Islam, N. Hossain, Z. Mahmud, T. Rayhan, N.J. Nishi, M. A. Chowdhury, Recent advances of additive manufacturing in implant fabrication – A review, *J. Alloys Comp.* **992** (2024) #174447.

[15] Y. Peng, M. Chen, J. Wang, J. Xie, C. Wang, X. Yang, X. Huang, Z. Gou, J. Ye, Tuning zinc content in wollastonite bioceramic endowing outstanding angiogenic and antibacterial functions beneficial for orbital reconstruction, *Bioactive Mater.* **36** (2024) 551–564.

[16] T. E. Pirnazarov, Numerical solution of a three-dimensional gas filtration problem in complex domains using component-wise splitting and streamwise sweep methods, *Problems Comput. Appl. Math.* **1** (2017) 11–17.

[17] P. Song , Q. Song, Z. Yang, G. Zeng, H. Xu, X. Li, W. Xiong, Numerical simulation and exploration of electrocoagulation process for arsenic and antimony removal: Electric field, flow field, and mass transfer studies, *J. Environ. Manag.* **228** (2018) 336–345.

[18] L. Xu, J. Fang, J. Pan, H. Qi, Y. Yin, Y. He, X. Gan, Y. Li, Y. Li, J. Guo, Zinc finger-inspired peptide-metal-phenolic nanointerface enhances bone-implant integration under bacterial infection microenvironment through immune modulation and osteogenesis promotion, *Bioactive Mater.* **41** (2024) 564–576.

[19] Y. Zhang, J. Deng, J. Chen, P. Yu, X. Xing, Leaching of zinc from calcined smithsonite using sodium hydroxide, *Hydromettallurgy* **131–132** (2013) 89–92.

[20] Y. Zhang, J. Deng, J. Chen, P. Yu, X. Xing, The electrowinning of zinc from sodium hydroxide solutionse, *Hydromettallurgy* **146** (2014) 59–63.

[21] T. A. Zhuaspayev, Streamwise sweep for the coefficient inverse problem of heat propagation in a material, *Izvestiya VUZov (Kyrgyzstan)* **5** (2012) 21–24.